www.ietdl.org

Published in IET Image Processing
Received on 29th July 2010
Revised on 7th September 2011
doi: 10.1049/iet-ipr.2011.0029

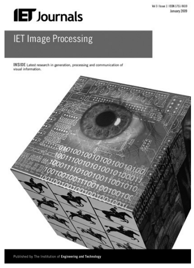

ISSN 1751-9659

Adaptive and efficient colour quantisation based on a growing self-organising map

W.-G. Teng[1] P.-L. Chang[2] C.-T. Yang[3]

[1]Department of Engineering Science, National Cheng Kung University, Tainan, Taiwan
[2]Department of Computing, Imperial College London, London, UK
[3]Department of Psychology and Institute of Cognitive Science, National Cheng Kung University, Tainan, Taiwan
E-mail: wgteng@mail.ncku.edu.tw

Abstract: Studies on colour quantisation have indicated that its applications range from the relaxation of displaying hardware constraints in early years to a modern usage of facilitating content-based image retrieval tasks. Among many alternatives, approaches based on neural network models are generally accepted to be able to produce quality results in colour quantisation. However, these approaches using n quantised neurons require $O(n)$ for a full search strategy, which is inefficient when n becomes large. In view of this, we propose to incorporate a growing quadtree structure into a self-organising map (GQSOM) which reaches a search time $O(\log n)$. Specifically, the strategy of inheriting from parent neurons hierarchically facilitates a much more efficient and flexible learning process. Both theoretical and empirical studies have shown that our approach is adaptive in determining an appropriate number of quantised colours, and the performance is significantly improved without compromise of the quantisation quality.

1 Introduction

Colour quantisation is a task to reduce the number of colours in an image while keeping this image as visually similar to the original one as possible. Such a process was significant in early years as personal computers at that time could usually display at most 256 different colours. For recent applications, colour quantisation is also a crucial preprocessing step in several image processing tasks, for example, image compression and image segmentation [1]. Moreover, colour quantisation can facilitate the indexing process for the emerging field of content-based image retrieval by identifying a number of representative colours in an image [2].

In previous approaches [1, 3–8], the number of colours to retain during the colour quantisation process is usually required to be predetermined. Nevertheless, it can be easily understood that the appropriate number of quantised colours varies with different image contents. The effectiveness of a colour quantisation approach can be assessed from the quantisation error of resulting images in addition to subjective evaluations on the quantisation quality. Consequently, we propose to devise a flexible approach in this paper so that colour images can be quantised up to a satisfactory quality level.

Prior works show that approaches based on neural network models, especially the self-organising map (SOM), are generally effective in colour quantisation tasks [5]. However, because of the long and repetitive learning process required for these neural network models, SOM is not a good candidate in handling numerous images in practice. In view of this, we elaborate on simplifying the learning process by introducing the quadtree structure in the SOM approach. Specifically, the number of neurons can grow at a rapid pace, that is, with the power of four, whereas the final number of neurons (and thus the number of quantised colours) can be made arbitrary. Moreover, the feature of neighborhood learning (NL) is not explicitly realised in our approach so that the efficiency can be further improved without the compensation of algorithm effectiveness. To demonstrate the adaptability, effectiveness and efficiency of the proposed approach, comparisons among other conventional approaches are made in our empirical studies.

The rest of this paper is organised as follows. Preliminaries and related works are briefly reviewed in Section 2. Details of the proposed approach are explored in Section 3. In Section 4, experiment studies are conducted to evaluate the performance of our approach. Finally, Section 5 contains the concluding remarks.

2 Preliminaries

For identifying representative colours in an image, the concept of psychovisual redundancy and common techniques for colour quantisation are reviewed in Section 2.1. Moreover, variant neural network models which can be utilised for colour quantisation are discussed in Section 2.2.

2.1 Psychovisual redundancy and colour quantisation

When displaying colour images, certain information contained in an image is of less significance to be perceived by human beings [9]. Such a phenomenon is not surprising as a true colour image contains 2^{24} colours, which are more than 16 million different colours and exceed the range of human perception. When neurons receive such a great amount of colour information, they cannot represent all information in the visual cortex because of the limited capacity. Thus, human visual system is evolved to transform the visual inputs as much as possible into a statistically independent basis to form a redundancy reduced representation [9, 10]. On the basis of the fact that the visual representation is redundancy reduced, if by removing certain colours, the reconstructed image can be perceived visually identical to the original one, the removed part is regarded as redundant colours. Consequently, it is usually possible to exploit fewer colours to represent an image with initially numerous colours once the ‘psychovisual redundancy’ [11] is reduced with a proper colour quantisation approach.

In prior studies, well-known approaches for colour quantisation include median-cut [12], octree [13], variation-based [4] and clustering-based algorithms [5]. The median-cut algorithm divides the colour space based on the distribution of original colours so that each partition contains roughly equal numbers of pixels. Then, representative colours are found by averaging the colours in each partition. This algorithm works efficiently but suffers from numerous quality problems, for example, large errors in handing a low-density part of the colour space. In contrast, octree partitions the three-dimensional colour space by recursively subdividing it into eight octants. This approach usually generates good partition results but tends to be relatively inefficient because of possible recursive examination of multiple children at each node. Moreover, the human visual perception to colour variation sensitivity is considered in a variation-based approach to generate representative colours. Finally, when colour quantisation is formulated as a clustering problem, the process is usually regarded as the generation of a codebook or a palette using three-dimensional vectors as a pixel contains three colour components. Specifically, the whole process consists of two stages, that is, generation of a colour palette and mapping of representative colours. Therefore it can be easily noted that the quality of generated colour palette is critical to the effectiveness of colour quantisation.

2.2 Utilising the self-organising map for colour quantisation

For colour quantisation, neural network models are widely used in prior works [1, 3, 5–8] to perform clustering of colour vectors. Specifically, the Kohonen SOM [14] is an unsupervised and competitive learning neural network which provides a way of projecting high-dimensional data to a lower-dimensional space while preserving as much as possible the similarities among these data. Thus, this approach is broadly used for data clustering and complex data visualisation.

The essential structure of SOM consists of an input layer and an output layer. A typical two-dimensional SOM with $M \times N$ output neurons is shown in Fig. 1, which is trained by p input data elements. The input data $\boldsymbol{X}_i$ and the weights of output neurons $\boldsymbol{w}_j$ are represented as d-dimensional vectors, that is, $\boldsymbol{X}_i = [x_1^i, x_2^i, \ldots, x_d^i]^{\mathrm{T}}$ for $i = 1, 2, \ldots, p$ and $\boldsymbol{w}_j = [w_1^j, w_2^j, \ldots, w_d^j]^{\mathrm{T}}$ for $j = 1, 2, \ldots, M \times N$. Note that the dimension d varies with applications, and must be consistent for both the input data and the weights of output neurons. For representing colours, three-dimensional vectors are sufficient.

SOM operates in two phases, that is, training and mapping. In each training iteration, one input data element is randomly selected and fed to the output layer. Among the output neurons, the one with weight vector most similar to the input is called the best-matching unit (BMU). The weights of the BMU and its neighbouring neurons are adjusted towards the input vector. Note that the magnitude of the change typically decreases with time and with distance from the BMU. This training phase ends when the weights of output neurons converge after a (usually large) number of iterations. Then, the mapping phase may begin so that each of the input data is mapped to the output neuron which is with the most similar weight vector. Consequently, the final output neurons act as a map to reflect the clustering result of the input data after the mapping phase is completed. For the task of colour quantisation, SOM-based approaches exhibit higher quality than several conventional algorithms [5]. However, technical difficulties are noted in the original model, including the inflexibility in the number of output neurons, sensitivity to parameter values and a long-time training process. Consequently, a number of improving techniques are proposed in recent studies.

The inflexible structure of a fixed neuron number in the output layer has been redesigned recently [3, 6]. Through a dynamically growing mechanism, the number of neurons can be adjusted correspondingly. However, as the search strategy for the BMU remains the same as the one used in the typical SOM, the other drawbacks are still unsolved. In contrast, some other efforts have been spent on reducing the sensitivity in parameter setting whereas achieving better quantisation results [1, 8]. Finally, note that the strategy for searching the BMU is the primary bottleneck to further improve the efficiency of the whole process. In the typical SOM, the search takes $O(n)$ where n is the number of neurons in the output layer. A progressive algorithm which

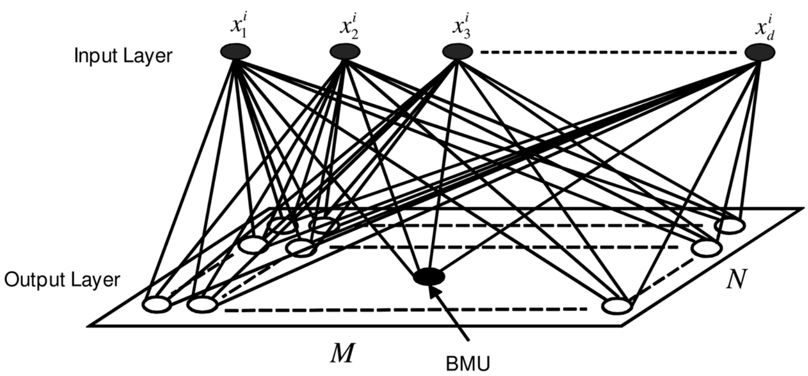

Fig. 1 *Typical SOM structured with the two-dimensional output layer*

IET Image Process., pp. 1–10
doi: 10.1049/iet-ipr.2011.0029

utilises the tree structure reduces this search complexity to $O(\log_s n)$ where s is the number of children per node in the tree structure [15]. Nevertheless, to the best of our knowledge, none of prior works try to benefit neural network model by coupling with all these improving techniques on the colour quantisation task.

3 Growing quadtree for SOM-based colour quantisation

The way the growing quadtree can be incorporated into the SOM approach is explored in Section 3.1. Moreover, details of our growing quadtree structure into a self-organising map (GQSOM) approach for colour quantisation are elaborated in Section 3.2.

3.1 Incorporating a growing quadtree structure into the SOM

Instead of using a fixed topology as the output layer (and therefore a fixed number of output neurons), our approach GQSOM utilises a growing quadtree structure to dynamically allocate an appropriate number of output neurons. For the task of colour quantisation, the collection of all pixels in the original image using a certain three-channel colour space is denoted by Ω. The input vectors are denoted as $\boldsymbol{X}_i = [x_1^i, x_2^i, x_3^i]^{\mathrm{T}}$, $\forall i \in \Omega$, and the weight vectors of a neuron are $\boldsymbol{w}_j = [w_1^j, w_2^j, \ldots, w_d^j]^{\mathrm{T}}$, $\forall j \in [\boldsymbol{X}_i, c]$. Thus, it is noted that the weight vector of an output neuron stands for a representative colour in our codebook.

Furthermore, the neighbourhood relationship in GQSOM is carefully re-examined. Specifically, the adopted quadtree structure may contain a number of layers as shown in Fig. 2. Each parent neuron on the quadtree, that is, neurons which are not on the bottom layer, can have at least one child neuron and at most four child neurons. Note that the quadtree grows by adding new child neurons to start a new layer 'only after' neurons in the current layer are all well trained. Also note that new child neurons inherit the weight vector from their parent neurons directly as their initial weight vectors.

During the learning process, if a neuron is frequently selected as the BMU of some input vectors, this neuron could be well trained and thus its weight vector should converge to steady values after numerous times of training. We thus propose to introduce this 'frequency-sensitive' feature [1] in our learning function. Moreover, the learning process of a neuron is designed to be independent of that of other neurons. Specifically, we choose to omit the neighbourhood relationship in the learning function so that

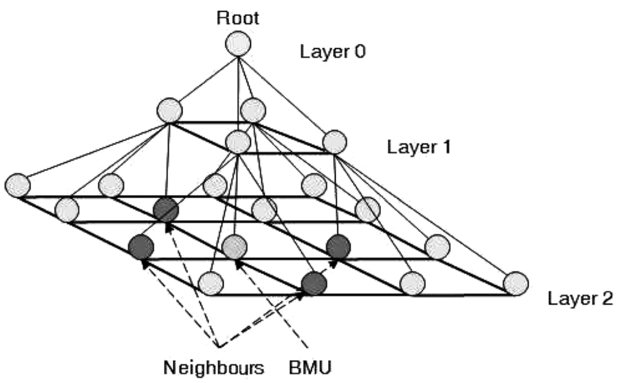

Fig. 2 *SOM with a growing quadtree structure*

the sibling neurons could be diverse enough to represent the dominant input vectors. This feature is especially critical in the very beginning since the number of neurons is limited in early layers. In our point of view, performing NL may result in a significant error of final quantisation results as the corresponding impact is accumulated through layers of the growing quadtree. This conclusion is further verified through our empirical studies. Corresponding details are presented in Section 4.2.

Deciding a proper stopping criterion to terminate the growing process is another crucial issue. For simplicity, GQSOM can stop growing the quadtree at some layer once acceptable quantisation quality has been achieved. Nevertheless, the drawback is that the number of output neurons must be the power of four as we have a complete quadtree. To relieve this difficulty, we scrutinise the growing process to make it sophisticated enough so that the number of output neurons can be made arbitrary. In other words, once the user specifies a desired number of quantised colours, our approach GQSOM can stop growing the quadtree when the number of output neurons reaches the specified value even if the quadtree is incomplete at that time.

3.2 Colour quantisation with GQSOM

To make the proposed GQSOM an adaptive approach, the learning and mapping processes are not separated as two disjointed parts in our algorithm. Also, either the maximum number of quantised colours K or the desired quantisation quality Q (usually in terms of some error metric) can be specified as a criterion. Details of our algorithm GQSOM are shown in Fig. 3.

Before illustrating how our algorithm works, a significant concept is firstly explored. Specifically, to reduce the search space required during the growing process, we devise to denote a candidate set of neurons for an input vector $\boldsymbol{X}_i$ as candidate $[\boldsymbol{X}_i]$. As shown in Fig. 2, only the child neurons of either the current BMU or its neighbours (i.e. the shaded nodes) are designed to be included in this candidate set candidate $[\boldsymbol{X}_i]$. As the quadtree grows, only a neuron contained in this candidate set can be the next BMU of $\boldsymbol{X}_i$ during the training process of the next layer. In other words, the maximum number of neurons needs to be searched is $(1 + 4) \times 4 = 20$ as there are at most four neighbours around the BMU and a neuron can have at most four child neurons. This implies that the search space remains limited as the number of neurons grows.

In the beginning of algorithm GQSOM as shown in lines 1–4 of Fig. 3, the quadtree structure contains only a root neuron whose weight vector is randomly initialised, that is, the number of layers $l = 0$. Obviously, candidate $[\boldsymbol{X}_i]$ contains only the root neuron, $\forall i \in \Omega$.

Next, the training process of a single layer is as shown in lines 6–10 of Fig. 3. Specifically, to reduce the impact of spatial dependencies among pixels in the original image, an input vector $\boldsymbol{X}_i$ is randomly selected to train the neurons. The BMU of $\boldsymbol{X}_i$ is selected from the candidate set candidate$[\boldsymbol{X}_i]$ according to (1).

$$\|\boldsymbol{X}_i - \boldsymbol{w}_{\mathbf{BMU}}\| = \arg\min||\boldsymbol{X}_i - \boldsymbol{w}_j||, \quad \forall j \in \text{candidate}[\boldsymbol{X}_i] \tag{1}$$

where $\|\ldots\|$ denotes the Euclidean distance. Note that if there are more than one neuron satisfying (1), then only one of them is randomly selected as the BMU. This BMU

doi: 10.1049/iet-ipr.2011.0029

Objective

Given a training set X_i, $\forall i \in \Omega$, where Ω is the collection of all pixels in the original image, generate an adaptive codebook with the specified size K or a certain size satisfying the specified quantization quality Q. Note that this algorithm works when either K or Q is specified.

Algorithm

1. The initial quadtree is with only a root neuron whose weight vector is randomly initialized.
2. Set all the candidate sets of neurons, i.e., *candidate[X_i]*, $\forall i \in \Omega$, to the root.
3. Set the number of layers $l = 0$.
4. Set the total number of nodes in the bottom layer *total_n_nodes=1* (i.e., the root neuron).
5. **While** (*total_n_nodes* $\leq K$) {

// Training process of a single layer
6. **Do** {
7. Determine the BMU of a randomly selected input vector X_i from its corresponding candidate set *candidate[X_i]* using Eq. (1)

$$\left\| \boldsymbol{X}_i - \boldsymbol{w}_{\mathbf{BMU}} \right\| = \arg\min \left\| \boldsymbol{X}_i - \boldsymbol{w}_j \right\|, \forall j \in candidate[\boldsymbol{X}_i] \tag{1}$$

where ||…|| denotes the Euclidean distance.
8. Increment the winning times of this BMU neuron, i.e., T_{BMU}.
9. Conduct the learning process on this BMU neuron using Eq. (2) which is the proposed learning function with the frequency-sensitive feature.

$$\boldsymbol{w}_{\mathbf{BMU}}(t+1) = \boldsymbol{w}_{\mathbf{BMU}}(t) \times \frac{T_{BMU}}{T_{BMU}+1} + \boldsymbol{X}_i(t) \times \frac{1}{T_{BMU}+1} \tag{2}$$

where t is the number of iteration, and T_{BMU} is the winning times of this neuron.
10. } **While** (There is at least one neuron which does not satisfy Eq. (3).);

$$\frac{1}{T_{BMU}+1} < \varepsilon \tag{3}$$

// Reset the BMUs for all input data and calculate the current quantization error
11. *q_error* = 0;
12. **For all** $i \in \Omega$ {
13. Determine the BMU of X_i from its corresponding candidate set *candidate[X_i]* using Eq. (1)
14. *q_error* = *q_error* + error calculated based on X_i and its BMU according to a pre-defined metric (e.g., the Euclidean distance);
15. }

// Check the stopping criteria
16. **If** ((*total_n_nodes* == K) or (*q_error* reaches the specified quality level Q)) {
17. **break;**
18. }

// Growing of the quadtree
19. Child neurons are grown one by one according to the variance of all X_i belonging to an identical parent neuron in descending order. This step works iteratively until the number of child neurons (i.e., *total_n_nodes*) reaches K or until all parent neurons have four child neurons. Note that the weights of child neurons are duplicated from the weights of their parent neurons.
20. **For all** $i \in \Omega$ {
21. Update the candidate set of X_i, i.e., *candidate[X_i]*, to include all the child neurons of either the corresponding BMU or its neighbor neurons;
22. }
23. $l = l + 1$;
24. }

Fig. 3 *Algorithm GQSOM for generating an adaptive codebook*

(or the winning neuron) then learns from X_i (i.e. to become more similar to X_i) using (2) which is the proposed learning function with the frequency-sensitive feature.

$$\boldsymbol{w}_{\mathbf{BMU}}(t+1) = \boldsymbol{w}_{\mathbf{BMU}}(t) \times \frac{T_{\mathrm{BMU}}}{T_{\mathrm{BMU}}+1} + \boldsymbol{X}_i(t) \times \frac{1}{T_{\mathrm{BMU}}+1} \tag{2}$$

where t is the number of iteration, and T_{BMU} denotes the winning times of this neuron. In contrast, the maturity degree of this BMU is evaluated using (3).

$$\frac{1}{T_{\mathrm{BMU}}+1} < \varepsilon \tag{3}$$

where ε is a small number depending on the scales of adopted

doi: 10.1049/iet-ipr.2011.0029

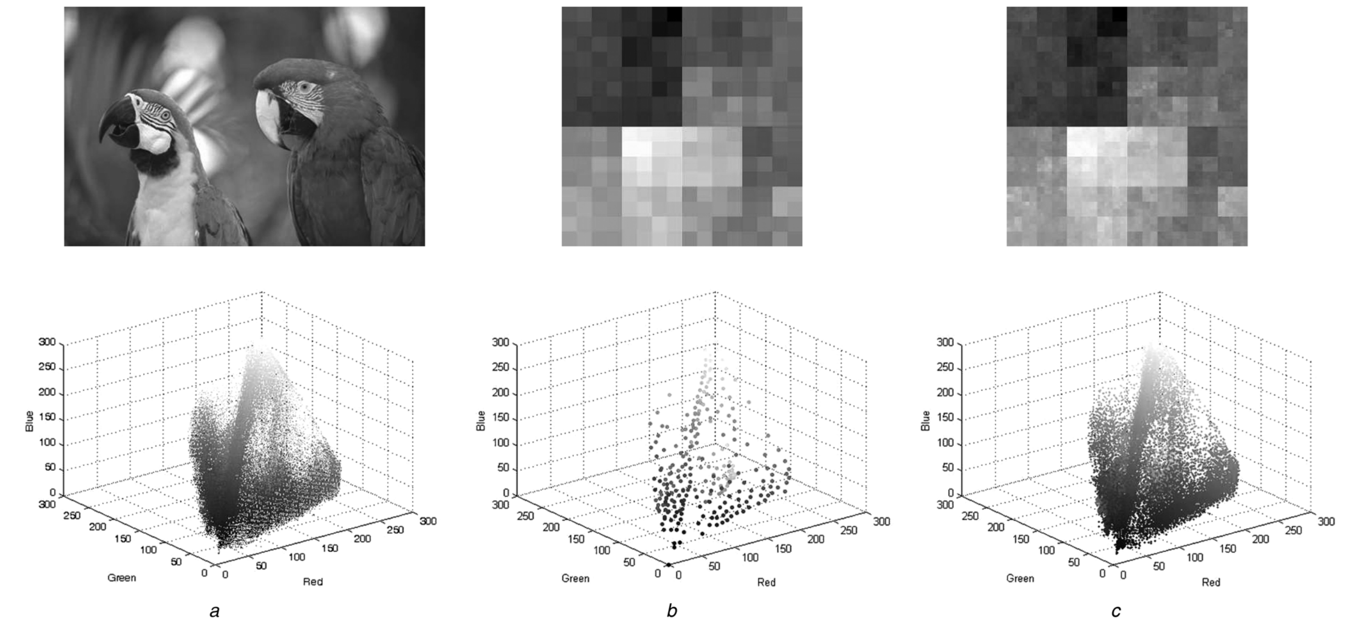

Fig. 4 *Colour palettes and corresponding colour distribution plots*

a Original image in 72 079 colours
b 256 colours generated by GQSOM
c 16 384 colours generated by GQSOM

colour spaces. For example, it is suggested to have ε smaller than 1 for RGB colours (i.e. 0–255) and have it smaller than 0.01 for Lab colours (i.e. 0.00–1.00). Intuitively, although the left part of (3) becomes sufficiently small, the corresponding impact of using (2) to learn from $\boldsymbol{X}_i$ could almost be neglected. When all the neurons become mature, the training process of the current layer is completed.

After the training process, all the input vectors are reexamined to determine the corresponding BMUs and the resulting quantisation error as shown in lines 11–15 of Fig. 3. Note that the weight vector of an output neuron stands for a representative colour in our codebook. Thus, the current quantisation error can be easily calculated by considering the distance between all the input vectors and their BMUs. Then, as shown in lines 16–18 of Fig. 3, the whole process stops if either the specified codebook size K or the desired quantisation quality Q is reached.

Once the stopping criteria are not met, the quadtree grows as shown in lines 19–23 of Fig. 3. Specifically, child neurons are grown one by one according to the variance of all $\boldsymbol{X}_i$ belonging to an identical parent neuron in descending order. That is, if there are several parent neurons, the one with the largest variance, as calculated based on all corresponding $\boldsymbol{X}_{i,}$ is the first one to grow a new child neuron. The parent neuron with the second largest variance is the next one, and so on. This step works iteratively until the number of child neurons (i.e. 'total_*n*_nodes') reaches K or until all parent neurons have four child neurons. The initial weights of child neurons are duplicated from the weights of their parent neurons. Then, all the candidate sets of neurons (candidate [$\boldsymbol{X}_i$], $\forall i \in \Omega$) are updated as a preparation for the training of the next layer. Finally, the number of layers is incremented, that is, $l = l + 1$, and the whole process starts over again.

After the whole process of algorithm GQSOM is completed, a corresponding codebook is obtained by directly using all the weight vectors of neurons in the bottom layer. The quantised image is then generated accordingly. To further clarify this concept, an example image with its colour distribution is shown in Fig. 4*a*. After conducting two different quantisation processes, the resulting codebooks containing 256 and 16 384 colours are shown in Figs. 4*b* and *c*, respectively. As expected, the one in Fig. 4*c* is with more similar colour distribution to that of the original image in Fig. 4*a*. Note that one may always expect to acquire a more subtle quantised colour image, as the codebook size increases.

4 Empirical studies

The experimental environment is firstly introduced in Section 4.1. Experimental results based on several different approaches for colour quantisation are reported in Section 4.2. To further evaluate the impacts on visual perception, a psychophysical experiment is conducted in Section 4.3. Moreover, we examine our approach GQSOM with a large dataset in Section 4.4.

4.1 Experimental environment

For comparison purposes, the proposed GQSOM approach and several other techniques, including the typical SOM, median-cut and an octree-based adaptive spatial subdivision algorithm [13], are all tested on a personal computer equipped with an Intel Pentium 4 3.4-GHz processor and 2.5-GB memory. All experimental programmes are implemented in Java. To evaluate the similarity of reconstructed images, the peak signal-to-noise ratio (PSNR) is used as an objective metric [11]. Specifically, the PSNR is calculated as shown in (4).

$$\mathrm{PSNR} = 10 \times \log\left(\frac{3 \times 255^2}{\mathrm{MSE}}\right) \qquad (4)$$

In addition, the MSE (i.e. mean squared error) is

$$\mathrm{MSE} = \frac{1}{N}\sum_{i=1}^{N} |\boldsymbol{X}_i - \boldsymbol{Y}_i|^2 \tag{5}$$

where N is the number of total pixels whereas $\boldsymbol{X}_i$ and $\boldsymbol{Y}_i$ are the vectors of the i-th pixel in the original and reconstructed images, respectively. It is commonly accepted that the higher PSNR value, the subtler quantised image is rendered. Without loss of generality, all images and their corresponding objective criteria in terms of the PSNR are manipulated in the RGB colour space if not mentioned explicitly.

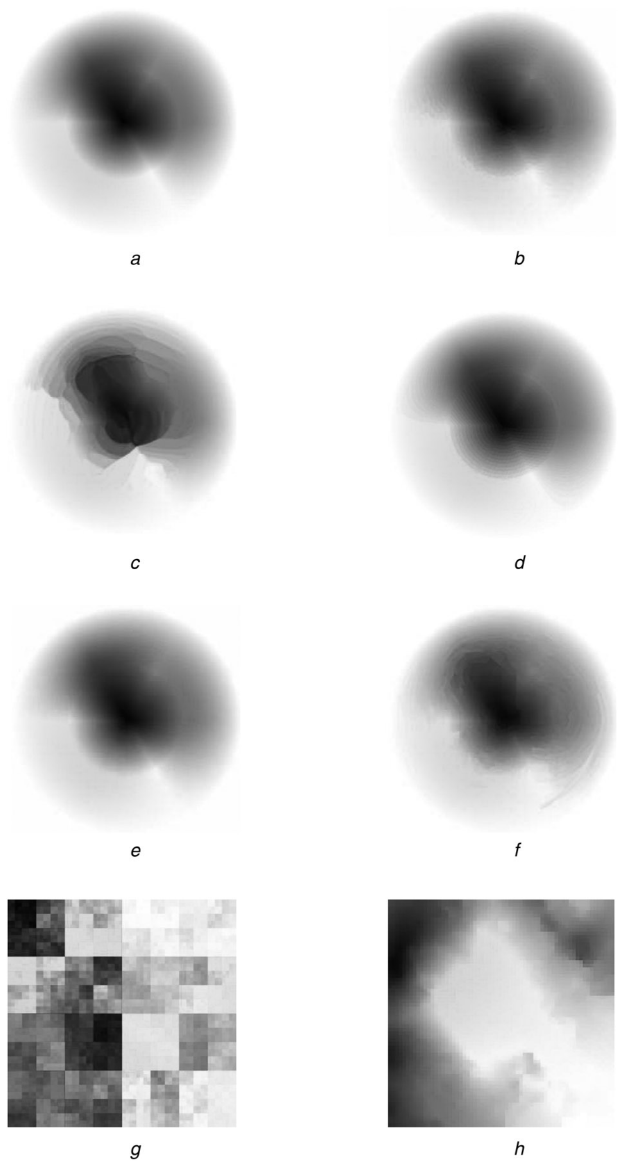

Fig. 5 *Quantisation results in 4096 colours of a colour wheel image*

a Original image
b Resulting image of SOM
c Resulting image of Median-cut
d Resulting image of Octree
e Resulting image of GQSOM
f Resulting image of GQSOM with NL
g Corresponding codebook of *e*
h Corresponding codebook of *f*

4.2 Performance of visual similarity

To evaluate the performance of our approach GQSOM, a synthetic image of the homogenous ‘colour wheel’ is firstly tested to simulate a critical situation for colour quantisation. As shown in Fig. 5*a*, this colour wheel originally consists of 152 241 colours. By applying different techniques for colour quantisation, the resulting images all contain nearly 4096 colours as shown in Figs. 5*b*–*f*.

In addition to the usage of PSNR as an objective indicator, the similarity evaluation of a reconstructed image can be directly conducted with some subjective judgment. It is thus observed from Figs. 5*e* and 6*a* that our approach GQSOM is with the best quantisation quality in this case. To verify the possible performance degradation of explicitly incorporating NL in GQSOM, an unsatisfactory result can be observed from Fig. 5*f*, although the corresponding palette in Fig. 5*h* is globally topology preservative. By comparing corresponding PSNR curves, that is, GQSOM and GQSOM + NL, in Fig. 6*a*, it is also reflected that NL incurs relatively poor quantisation results. In contrast, the typical SOM presents an underutilisation of neurons as observed from its PSNR curve in Fig. 6*a*, and its inefficiency as shown in Fig. 6*b*.

As shown in Fig. 6*b*, median-cut is generally the fastest approach. However, the quantisation result is not satisfactory

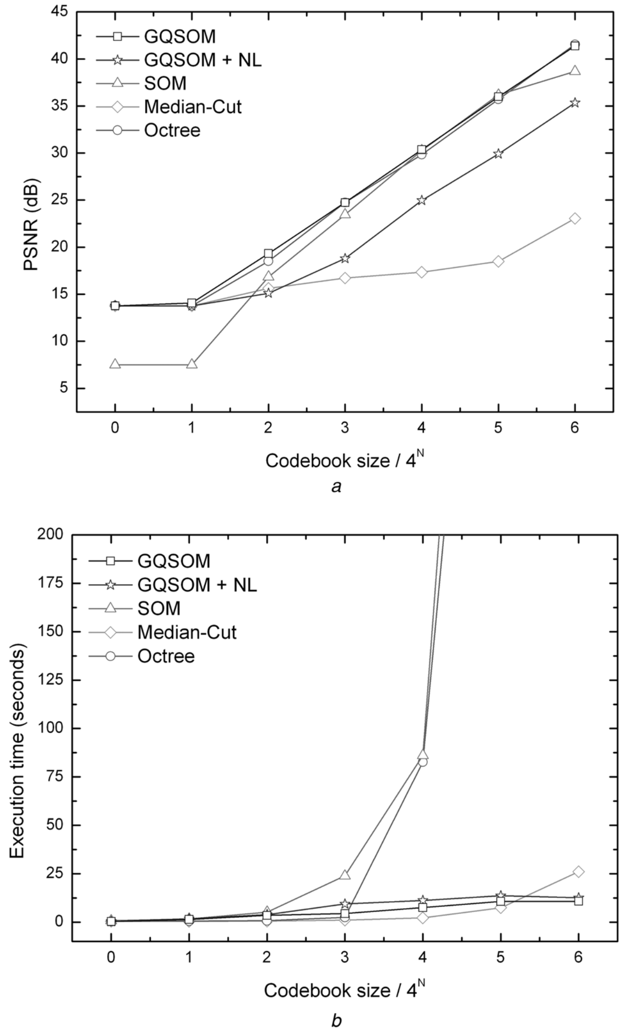

Fig. 6 *Performance of various approaches for quantising a colour wheel image*

a Quantisation quality in PSNR
b Execution time

doi: 10.1049/iet-ipr.2011.0029

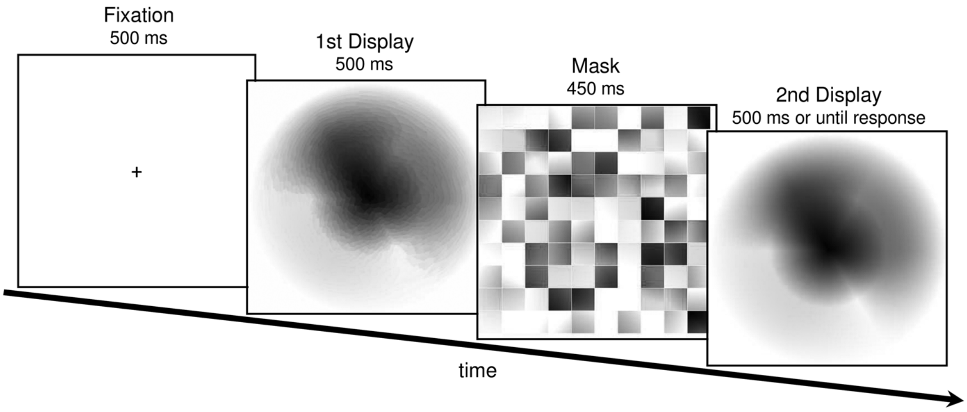

Fig. 7 *Illustration of the experimental procedure used in the psychophysical experiment*

In the beginning of each trial, a fixation is presented for 500 ms. After the fixation, a display is presented for 500 ms. Following a Modrian mask of 450 ms, another display is presented for 500 ms. Participants have to choose whether the first or the second image matches the original colour wheel as accurately as possible

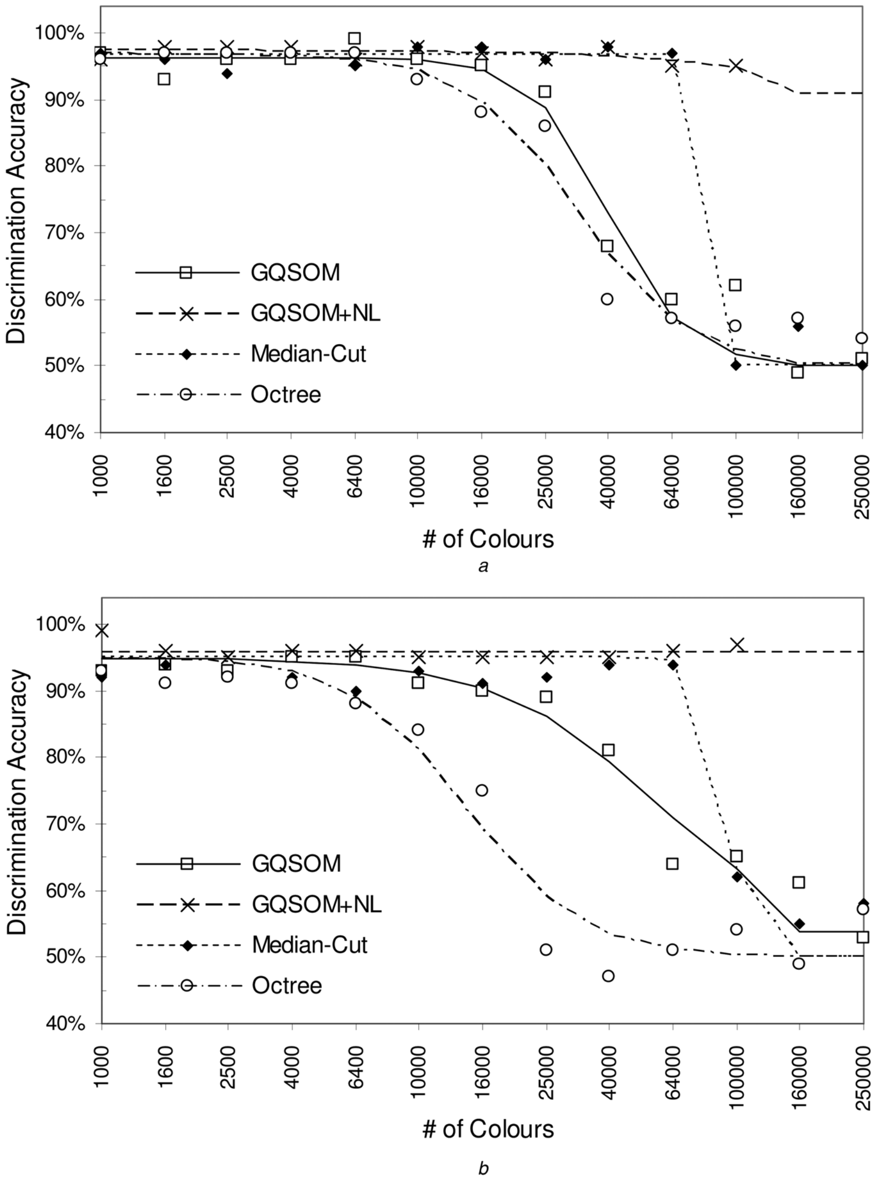

Fig. 8 *Plots of the discrimination accuracy as a function of the number of colours for*

a Observer YJC
b Observer WCJ
Each type of symbol and line, respectively, represents the observed data and modeling results for the four approaches: GQSOM, GQSOM + NL, median-cut and octree. Results from these two observers show that the psychometric functions gradually shift to the right. This trend starts from octree, GQSOM, median-cut, to GQSOM + NL

using either a subjective or an objective criterion. In Fig. 5*c*, the quantised colour wheel is apparently dissimilar to the original one even though a large number of 4096 quantised colours is utilised. Also, its PSNR performance in Fig. 6*a* is generally the worst. In contrast, the octree-based algorithm is generally with a good quality, whereas its execution time increases dramatically. It is also noted that the quantised image as shown in Fig. 5*d* is with some apparent circle effect due to the algorithmic property of octree.

4.3 Evidence from a psychophysical experiment

To further evaluate the impacts on visual perception, a 'psychophysical' experiment using a method of constant stimuli is conducted [16]. Specifically, this experiment is to measure human's subjective feelings on differences between the original and the quantised colour wheels. Generally speaking, when using a better quantisation technique and/or more colours for quantisation, the quantised image is more similar to the original one, such that observers are more difficult to distinguish between two images.

Empirical data are collected by sampling observers' performance at a number of different stimulus levels. By fitting the observed data with the psychometric function, the modelling results can describe the dependence of an observer's discrimination performance on the physical differences as a result of colour quantisation. The psychometric function $\psi(x)$, which specifies the relationship between the underlying probability of a correct response and the differences between the original and quantised images, x, is

$$\psi(x, \alpha, \beta, \gamma, \lambda) = \gamma + (1 - \gamma - \lambda)F(x, \alpha, \beta) \qquad (6)$$

where γ usually represents chance performance and is fixed at 0.5 in a two-interval-forced choice (2IFC) task, and λ represents the stimulus-independent error rate or lapse rate. The parameters α and β, respectively, represent the location and scale of the logistic function (F) (see [17, 18] for more details). The more the differences between the original and the quantised images (a decrement in x), the better the discrimination performance is. In other words, it is expected that the 'discrimination accuracy' $\psi(x)$ decreases as x gets larger.

Two observers (students named YJC and WCJ at National Cheng Kung University) volunteer this experiment. A 2IFC is performed (see Fig. 7 for the experimental procedure). After sequential presentation of two images, in which one is the original image and the other is the quantised image, observers are required to judge which one is the original one as accurately as possible while response time is not emphasised. Note that the presentation order of two images is counterbalanced.

Depending on the number of colours used for colour quantisation, the quantised images are divided into 13 levels which contains 265 trials for each level (number of colours in a log-scale: 1000, 1600, 2500, 4000, 6400, 10 000, 16 000, 25 000, 40 000, 64 000, 100 000, 160 000, and 250 000) for all the approaches of GQSOM, GQSOM + NL, median-cut and octree. Note that owing to the intrinsic property of topology preserving, the SOM approach is not capable to generate a quantised image with more than a few thousands of colours for our colour wheel, and is thus excluded in this experiment. When more colours are used for quantisation, the quantised image is more similar to the original one, such that observers are more difficult to distinguish between two images. As a result, we should find the discrimination accuracy decreases as a function of the increase of the number of colours used for quantisation. The rationale to compare between four approaches is that if an approach is better than the other, this approach can use fewer numbers of colours to represent the original image. Specifically, a method which has a psychometric function in the lower left of the figure is better than the other which has a psychometric function in the upper right of the figure. Therefore results from the psychophysical experiment can provide direct measurements on the evaluation of different colour quantisation approaches.

The observed and modelling results of the two observers are shown in Fig. 8. The symbols represent the observed data and the lines represent the modelling results fitted with the psychometric function. The two observers have shown the same pattern of results. By visual inspection, psychometric functions of octree and GQSOM are in the lower left of the figure, whereas those of median-cut and GQSOM + NL are in the upper right, suggesting that the former two approaches are better ones. We then conduct pair-wise t tests to examine whether two functions are significantly different from each other. Results show that the psychometric function of octree is significantly different from that of GQSOM ($P < 0.005$), and these two methods are significantly different from median-cut ($P < 0.0001$) which in turn is significantly different from GQSOM + NL

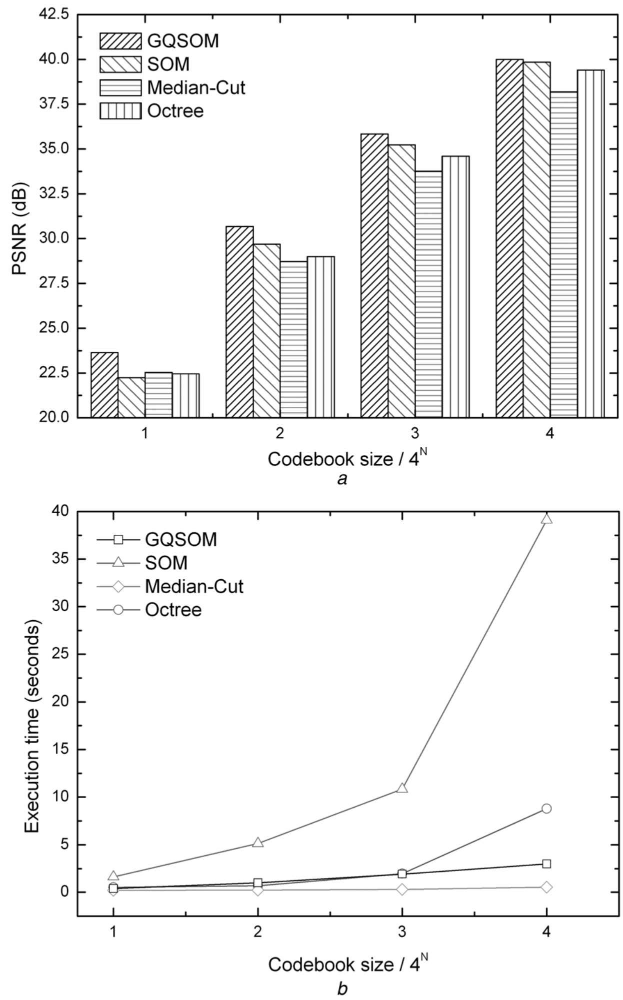

Fig. 9 *Performance of various approaches for quantising general colour images*

a Quantisation quality in PSNR
b Execution time

doi: 10.1049/iet-ipr.2011.0029

Fig. 10 *Comparison of two original images and their 64-colour quantised results using four different approaches, that is, GQSOM, SOM, median-cut and octree*

a Two subway construction workers (with originally 58 860 colours)
b Blooming cactuses (with originally 44 440 colours)

($P < 0.0001$). Therefore the results of this experiment suggest that the quantisation approaches from the best to the worst in rank are octree, GQSOM, median-cut and GQSOM + NL.

4.4 Colour quantisation in general cases

To further investigate the performance of different techniques for colour quantisation, a larger dataset [19] containing several categories of natural images is then used as our test bed. Each image of this dataset is with 481×321 pixels and 300 colour images in diverse context are randomly chosen for conducting our experiments. Specifically, the performance of adopting 4, 16, 64 and 256 quantised colours in terms of the PSNR values and the execution time are shown in Fig. 9. Moreover, a part of the 64-colour quantised results is shown in Fig. 10 to help illustrating the impact on quantisation quality when utilising different approaches. As summarised from the results of these experiments through different aspects, our approach GQSOM is with competitive advantages on both quantisation quality and computation efficiency.

5 Conclusions

In this work, we have focused on the development of a feasible approach for colour quantisation, a problem with great significance in several applications. In view of the inefficiency of neural network models, we have incorporated a growing quadtree structure to the SOM in our approach, called GQSOM. Empirical studies have shown that the quantised images generated by GQSOM exhibit, in general, the best quality as compared with those produced by several other alternative techniques, in terms of both objective and subjective criteria (i.e. the PSNR and a psychophysical experiment.) Moreover, the execution time required for GQSOM compares favourably with that required by the other techniques.

6 Acknowledgments

The authors thank Chia-Jung Wu and Ya-Shin Chian for their help in conducting the experiments. Also, the authors are supported in part by the National Science Council, Project No. NSC98-2221-E-006-164-MY2, Taiwan, R.O.C.

7 References

1 Chang, C.-H., Xu, P., Xiao, R., Srikanthan, T.: 'New adaptive color quantization method based on self-organizing maps', *IEEE Trans. Neural Netw.*, 2005, **16**, (1), pp. 237–249

2 Wong, K.-M., Po, L.-M., Cheung, K.-W.: 'A compact and efficient color descriptor for image retrieval'. Proc. 2007 IEEE Int. Conf. on Multimedia and Expo., July 2007, pp. 611–614

3 Atsalakis, A., Papamarkos, N.: 'Color reduction and estimation of the number of dominant colors by using a self-growing and self-organized neural gas', *Eng. Appl. Artif. Intell.*, 2006, **19**, (7), pp. 769–786

4 Chang, Y.-C., Lee, D.-J.: 'Color image quantization using color variation measure'. Proc. IEEE Symp. on Computational Intelligence in Image and Signal Processing, April 2007, pp. 127–132

5 Dekker, A.: 'Kohonen neural networks for optimal colour quantization', *Netw. Comput. Neural Syst.*, 1994, **5**, (3), pp. 351–367

6 Kirk, J.S., Chang, D.-J., Zurada, J.M.: 'A self-organizing map with dynamic architecture for efficient color quantization'. Proc. Int. Joint Conf. on Neural Networks, July 2001, pp. 2128–2132

7 Papamarkos, N., Atsalakis, A.E., Strouthopoulos, C.P.: 'Adaptive color reduction', *IEEE Trans. Syst. Man Cybern.*, 2002, **32**, (1), pp. 44–56

8 Wang, C.-H., Lee, C.-N., Hsieh, C.-H.: 'Sample-size adaptive self-organization map for color images quantization', *Pattern Recognit. Lett.*, 2007, **28**, (13), pp. 1616–1629

9 Atick, J.J., Li, Z., Redlich, A.N.: 'Understanding retinal color coding from first principles', *Neural Comput.*, 1992, **4**, (4), pp. 559–572

10 Caywood, M.S., Willmore, B., Tolhurst, D.J.: 'Independent components of color natural scenes resemble VI neurons in their spatial and color tuning', *J. Neurophysiol.*, 2004, **91**, (6), pp. 2859–2873

11 Gonzalez, R.C., Woods, R.E.: 'Digital image processing' (Pearson Prentice Hall, 2007, 2nd edn.)

12 Heckbert, P.: 'Color image quantization for frame buffer display', *ACM SIGGRAPH Comput. Graph.*, 1982, **16**, (3), pp. 297–307

13 Imagemagick, available at http://www.imagemagick.org/

14 Kohonen, T.: 'The self-organizing map', *Proc. IEEE*, 1990, **78**, (9), pp. 1464–1480

15 Koikkalainnen, P.: 'Progress with the tree-structured self-organizing map'. Proc. 11th European Conf. on Artificial Intelligence, August 1994, pp. 211–215

16 Klein, S.A.: 'Measuring, estimating, and understanding the psychometric function: a commentary', *Percept. Psychophys.*, 2001, **63**, (8), pp. 1421–1455

17 Wichmann, F.A., Hill, N.J.: 'The psychometric function: i. fitting, sampling, and goodness of fit', *Percept. Psychophys.*, 2001, **63**, (8), pp. 1293–1313

18 Wichmann, F.A., Hill, N.J.: 'The psychometric function: ii. bootstrap-based confidence intervals and sampling', *Percept. Psychophys.*, 2001, **63**, (8), pp. 1314–1329

19 Martin, D., Fowlkes, C., Tal, D., Malik, J.: 'A database of human segmented natural images and its application to evaluating segmentation algorithms and measuring ecological statistics'. Proc. Eighth IEEE Int. Conf. on Computer Vision, July 2001, pp. 416–423

doi: 10.1049/iet-ipr.2011.0029